doi:10.1016/j.ultrasmedbio.2004.01.005

ELSEVIER

● *Original Contribution*

ULTRASOUND-INDUCED CELL MEMBRANE POROSITY

CHERI X. DENG,* FRED SIELING,*† HUA PAN*† and JIANMIN CUI*†

*Department of Biomedical Engineering and †Cardiac Bioelectricity Research and Training Center, Case Western Reserve University, Cleveland, OH, USA

Abstract—Recent studies of ultrasound (US) methods for targeted drug delivery and nonviral gene transfection revealed new, advantageous possibilities. These studies utilized US contrast agents, commonly stabilized microbubbles, to facilitate delivery and suggested that US delivery resulted from cell sonoporation, the formation of temporary pores in the cell membrane induced by US. Using voltage clamp techniques, we obtained real-time measurements of sonoporation of single *Xenopus* oocyte in the presence of Optison™, an agent consisting of albumin-shelled C_3F_8 gas bubbles (mean diameter 3.2 μm). Ultrasound increased the transmembrane current as a direct result of decreased membrane resistance due to pore formation. We observed a distinct delay of sonoporation following US activation and characteristic stepwise increases of transmembrane current throughout US duration. We discovered that the resealing of cell membrane following US exposure required Ca^{2+} entering the cell through US-induced pores. (E-mail: cxd54@cwru.edu)   © 2004 World Federation for Ultrasound in Medicine & Biology.

Key Words: Sonoporation, Cell membrane, Ultrasound contrast agent, Drug delivery, Gene delivery.

INTRODUCTION

It has been demonstrated that microbubble ultrasound (US) contrast agents (UCAs) increased delivery efficiency of drugs and genes into cells using US (Miller et al. 1999, 2002; Bao et al. 1998; Greenleaf et al. 1998; Ward et al. 2000). However, it remains a challenge to achieve consistent, controllable delivery outcome because the mechanism and processes of sonoporation have not been clearly understood (Tachibana et al 1999). Due to the lack of methods for real-time monitoring of sonoporation at the cellular level, the efficiency of drug/gene delivery and sonoporation-associated side effects, such as loss of cell viability and enhanced apoptosis (Feril et al. 2003), have been studied only through post-US exposure analyses. A recent report demonstrated dynamic vesicle deformation and lysis due to microstreaming and strain induced by a low-amplitude bubble oscillation (Marmottant and Hilgenfeldt 2003). Although it is hypothesized that cavitation or violently collapsing bubbles may mechanically rupture cell membrane to induce sonoporation, allowing entry of DNA and macromolecules into the cell, it has been difficult to delineate the direct effects of UCA from the effects due to the subsequent bubble activities after UCA destruction (Feril et al. 2003).

To investigate the dynamics of sonoporation, we employed voltage clamp techniques (Fig. 1) to measure in real-time the transmembrane current of a single *Xenopus* oocyte during US irradiation in the presence of Optison™. *Xenopus* oocytes have been used to study membrane proteins such as ion channels and neurotransmitter receptors (Shi et al. 2002; Masu et al. 1987). Under voltage clamp, changes in the transmembrane current amplitude reflect directly the changes in cell membrane conductance and, therefore, can provide sensitive indications of the formation and subsequent resealing of pores in the cell membrane.

MATERIALS AND METHODS

Xenopus oocytes preparation

The animal protocol for *Xenopus* oocytes preparation is approved by the Institutional Animal Care and Use Committee at Case Western Reserve University. Adult female *Xenopus laevis* (NASCO, Fort Atkinson, WI) was anesthetized by immersion in 0.3% tricaine (Sigma, St. Louis, MO) solution for 20 min. Oocytes were taken from a small incision (0.5 to 1 cm), which was then sutured back. The toad was allowed to recover

Two-Microelectrode Voltage Clamp
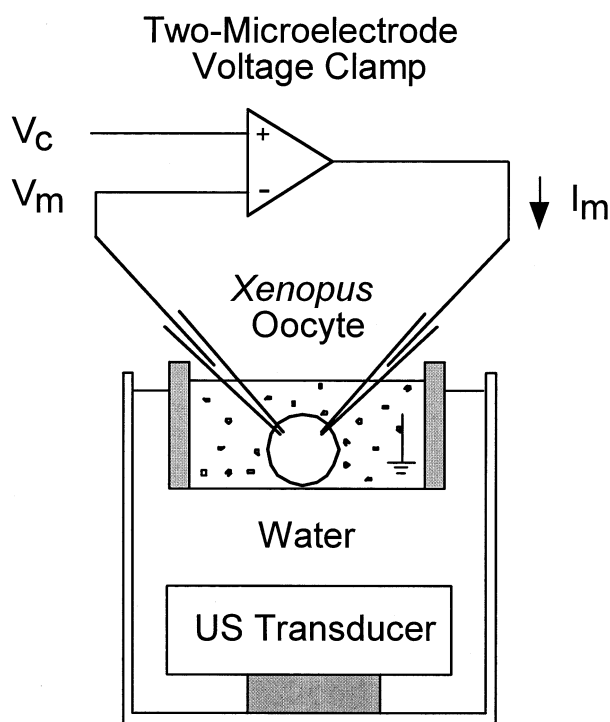
Fig. 1. The experimental setup for monitoring and characterization of sonoporation of the plasma membrane of *Xenopus* oocytes. Membrane potential of the oocyte (V_m) is clamped to be the same as the command potential (V_c). I_m = ionic current flowing through the plasma membrane. Oocyte in recording chamber bathed in ND96 or Ca^{2+}-free ND96 containing Optison™. The recording chamber bottom is acoustically transparent thin plastic film.

in fresh water. Oocytes were digested in collagenase (2 mg/mL in ND96 solution) for defolliculation. They were used immediately in experiments or stored in ND96 at 18°C for 1 or 2 days before use. ND96 contains (mM) 96 NaCl, 2 KCl, 1.8 $CaCl_2$, 1 $MgCl_2$, 5 HEPES, pH 7.60.

Ultrasound and electrophysiology

A single *Xenopus* oocyte was bathed in ND96 or Ca^{2+}-free ND96 (in mM: 96 NaCl, 2 KCl, 1 $MgCl_2$, 5 EGTA, 5 Hepes, pH 7.6) solutions. The membrane potential of the oocyte was clamped at −50 mV during recordings unless otherwise indicated, using a two-microelectrode voltage clamp amplifier (Dagan CA-1B, Dagan Corp., Minneapolis, MN) (Stuhmer 1998) (Fig. 1). Optison™ (~10^9 particles/mL) (Molecular Biosystems Inc., San Diego, CA) diluted in either ND96 or Ca^{2+}-free ND96 solution was added directly into the bath or through perfusion. Figure 1 shows the experimental setup. The cylindrical chamber, which has a radius of 1.5 cm and depth of 0.3 cm, has an acoustically transparent thin plastic film at the bottom, which was

submerged in water, allowing acoustic coupling and minimum interruption of US transmission and irradiation of the cell. A single oocyte of diameter of ~0.8 mm was deposited directly on the plastic film and was fixed by two microelectrodes inserted into its membrane. A circular planar piezoelectric lead zirconate-titanate (PZT) US transducer of a diameter of 5.1 cm (center frequency of 0.96 MHz) was vertically directed upward to the cell in the chamber at a distance of 2 cm. US activation and duration were synchronized using trigger signals from the voltage clamp for recording of the transmembrane current, permitting capture of the cell membrane status before, during, and after US irradiation in real-time. Tone burst pulses of US exposures were used in our experiments. The acoustic pressure amplitude of propagating US was predetermined from the output acoustic power measured using a US power meter (UPM-DT-10, Ohmic Instrument Co., Easton, MD). The actual maximum pressure was increased to a maximum of 2 times because of standing wave established due to the solution-air interface.

RESULTS

Figure 2a shows that, during voltage clamp of the membrane potential at −50 mV, the transmembrane current remained unchanged when neither US nor Optison™ was applied. No transmembrane current change was observed (Fig. 2b) in the absence of Optison™, even at US pressures up to 1.2 MPa. However, we observed consistently increases in the transmembrane current flowing into the cell with US exposure in the presence of Optison™ dilutions (0.05 ~ 5%). Figure 2c shows the inward transmembrane current for 1-s US exposure at 0.24 and 0.39 MPa. These pressure amplitudes are spatial-averaged positive peak pressures and are assumed to be equivalent to negative peak pressures under our experimental situations (Greenleaf et al. 1998). Figure 2c also shows that the transmembrane current recovers to the original level after the US exposure, representing the resealing process of the pores. The maximum current amplitude achieved during sonoporation represents the maximum extent of membrane disruption, which increases with Optison™ concentration, US pressure amplitude and US duration. Figure 3 shows the maximum current increase as a function of the acoustic pressure and duration. The error bars in Fig. 3 are standard error of means from $n = 4$ oocytes, except for the far right-hand bar when $n = 1$. For durations longer than 0.5 s at this pressure amplitude (0.6MPa), cell death (discolouration of the animal pole, irregular/disrupted membrane, large leaking current under voltage clamp and no response to US) is commonly seen.

a

No US, no CA

b

US, no CA

c

US, CA

0.24 MPa
0.39 MPa
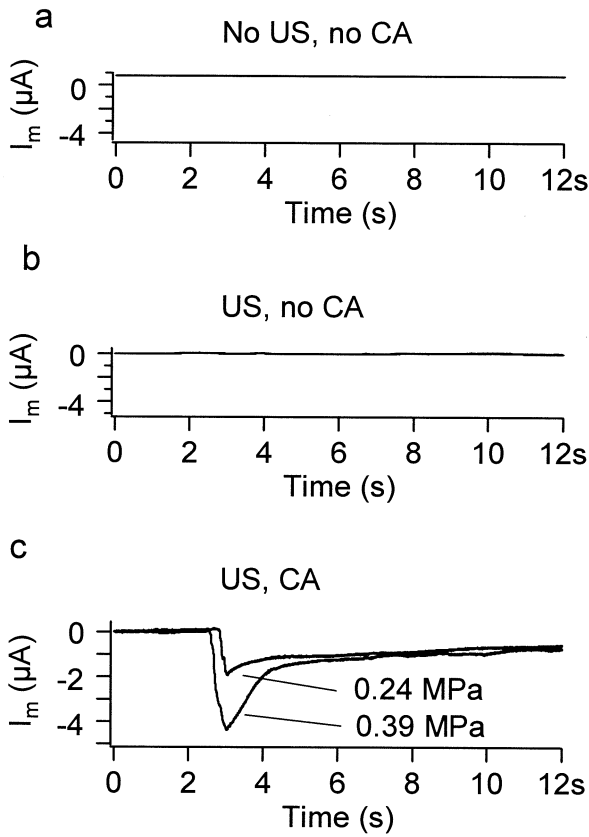
Fig. 2. US (tone burst pulse) induces ionic currents across the membrane in the presence of contrast agent (CA) Optison™ . The inside of the cell was clamped at –50 mV with respect to the grounded bath. Control experiments. (a) No US, no CA; (b) US ($<$ 0.8 MPa), no CA. (c) Downward currents caused by currents flowing into the cell when exposed to US with CA present.

We observed a distinct delay for the onset of transmembrane current increase after US (0.2 s at 0.23 MPa) activation in the presence of Optison™ (5%), depicted in Fig. 4. To further demonstrate this observation, Fig. 5
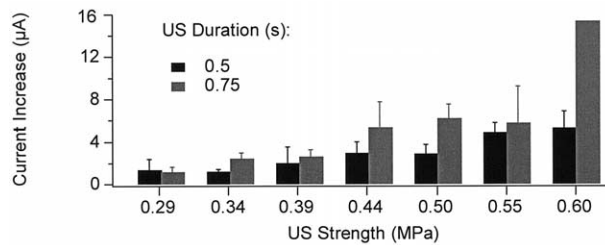
Fig. 3. Inward current induced by US increases with US duration (tone burst) and strength. $n = 4$, except $n = 1$ for the far right-hand bar. Black bars = results for US duration of 0.5 s, and gray bars = US duration of 0.75 s.
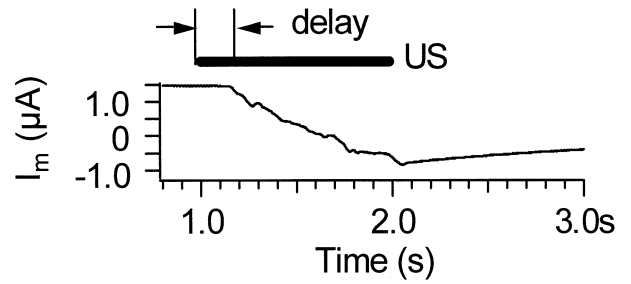
delay
US

Fig. 4. Delay of sonoporation is observed for the occurrence of current change after US activation. The US duration (tone burst) is 1 s and is activated at t = 1 s. Ionic current across the membrane changes after a delay (0.2 s) following the onset of US (0.29 MPa).

shows no change in transmembrane current in response to US exposure shorter than 0.2 s. Increase in inward transmembrane current was only observed when US duration exceeded 0.25 s, demonstrating that the initial disruption of Optison™ is not sufficient to induce sonoporation. Our systematic measurements indicate that the delay is longer at lower acoustic pressures and when the

a

100 ms

b

200 ms

c
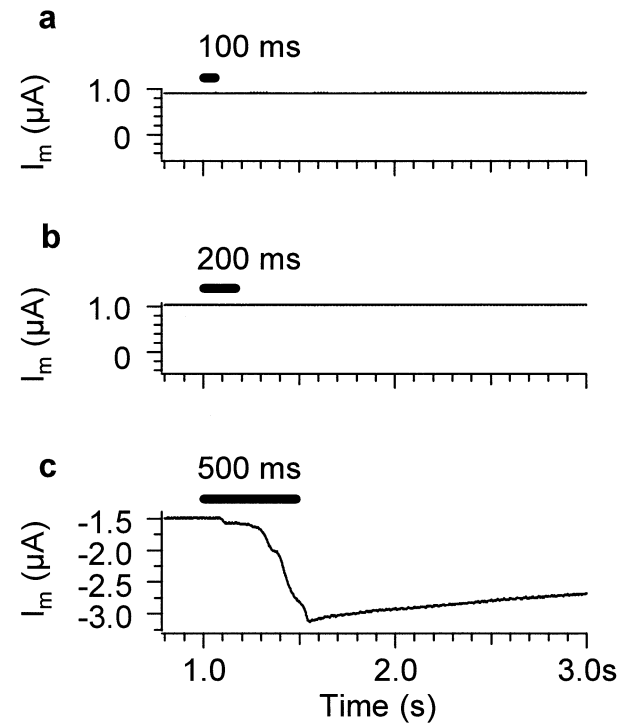
500 ms

Fig. 5. Short-time US irradiation (tone burst) cannot cause sonoporation of the plasma membrane. US of 0.24 MPa induced inward current at duration of 500 ms (c) but not at durations of 100 or 200 ms (a), (b). Oocytes were bathed in degassed ND96 solutions.
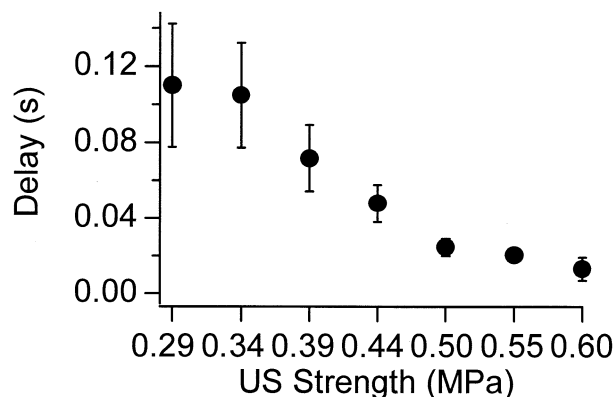
Fig. 6. Delay of sonoporation decreases with increasing tone burst US amplitude. Oocytes were bathed in degassed ND96 solutions.

Fig. 7. Steps in sonoporation of the plasma membrane. (a) Ionic current across the membrane changes with distinct steps. The oocyte bathed in Ca^{2+}-free ND96 in the presence of Optison™ was irradiated with tone burst US of 0.29 MPa and 1-s duration. (b) Histograms of steps duration under tone burst US of 0.24 MPa. Bin width is 0.035 s. In these experiments, the bath solution was saturated with air.

solution is degassed for 30 min before experiments. Figure 6 plots the delay as a function of the acoustic pressure for cells in air-saturated solutions with Optison™. At 0.29 MPa, the delay is about 0.1 s. At 0.6 MPa, the delay is shorter, about 0.02 s. The delay length levels off at 0.015 s when the acoustic pressure is higher than 0.7 MPa (data not shown).

We observed that, throughout the US duration, the inward transmembrane current continued to increase until the end of US duration (Figs. 2 and 4), an indication of sustained bubble activities during the US irradiation. Close examination of the current traces reveals that the inward transmembrane current increased in a characteristic stepwise fashion. The steps were more clearly demonstrated in recordings using Ca^{2+}-free ND96 solution (Fig. 7a), which excluded currents flowing through endogenous Ca^{2+}-dependent Cl^- channels that would have been activated by Ca^{2+} entering the cell during sonoporation (Miledi 1982; Barish 1983). Figure 7b shows the histograms of the step durations at 0.24 MPa (0.09 ± 0.25 s) in air-saturated solution with Optison™ (5% dilution), which is close to the duration of the delay at similar US strength (Fig. 6). These results suggest that the same physical process underlies the initial delay and the time lapse between consecutive steps.

Figure 8a shows serial transmembrane current traces recorded from the same oocyte in ND96 solution; each recording was obtained using 0.5-s US exposure in the presence of 5% Optison™. The cell membrane completely recovered after each US exposure and the transmembrane current returned to its initial amplitude of −4.5 μA at t = 0 s, shown at the beginning of each trace (Fig. 8a). The time course of recovery for all the traces can be fitted by a single exponential (Fig. 8a). The recovery rate does not vary significantly with US parameters or the maximum amplitude of the transmembrane current achieved during sonoporation (Fig. 8b). Figure 8b shows that the time constants are within 3 s (2.2 ± 1.3 s) range.

For cells bathed in Ca^{2+}-free ND96 solution, we discovered that the membrane did not show resealing after sonoporation. Figure 9a shows a series of transmembrane current traces obtained from an oocyte; Optison™ (5%) was added before each 0.5-s US exposure for each trace obtained. The transmembrane current amplitude exhibited an initial and small decay at the end of US exposure, but remained close to the peak (negative) value. The inward current maintained at the same level for minutes until the next US exposure with replenished Optison™, which caused its further increase.

To examine if Ca^{2+} entering the cell during sonoporation is important for membrane resealing, we recorded the US-induced current in ND96 solution at membrane potentials of either −50 or +50 mV. At −50 mV, extracellular Ca^{2+} flows in the direction of the electrical field and enters the cell through the US-induced pores, and the membrane resealed. At 50 mV, on the other hand, Ca^{2+} flows out of the cell. Either −50 or

a

in ND96

b
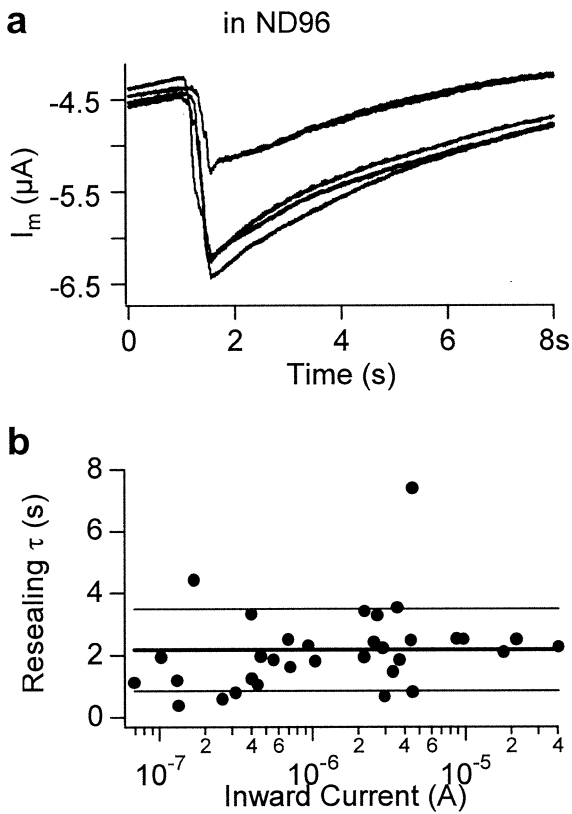
Fig. 8. Recovery of the plasma membrane from sonoporation. (a) Ionic currents across the membrane decay after sonoporation in ND96. Inward current traces were recorded from the same oocyte under repeated tone burst US irradiation of 0.29 MPa and 0.5 s duration. Fresh Optison™ was introduced before each US irradiation. (b) Resealing time constant τ was obtained by fitting the current decay with a single exponential and plotted against the maximum current amplitude under various US parameters and Optison™ concentration in ND96 solutions. (thick line) = the mean (2.17 s); (thin lines) = 1 SD (1.33 s) from the mean.

+50 mV clamp potential was used for the traces 1 to 5 in Fig. 10; the traces were obtained consecutively from trace 1 to trace 5. At −50mV (traces 1, 4, and 5), note the decay of the current traces and the lack of accumulated current increase at the beginning of trace 5. On the other hand, at +50 mV, little Ca^{2+} might enter the cell through the pores because of the adverse electrical field direction, and the membrane did not reseal (Fig. 10, traces 2 and 3; note the absence of decay of the current traces and the accumulated current increase at the beginning of trace 3).

DISCUSSION AND SUMMARY

Using two-electrode voltage clamp technique, we obtained real-time measurement of sonoporation of single *Xenopus* oocyte exposed with tone-burst US at 0.96
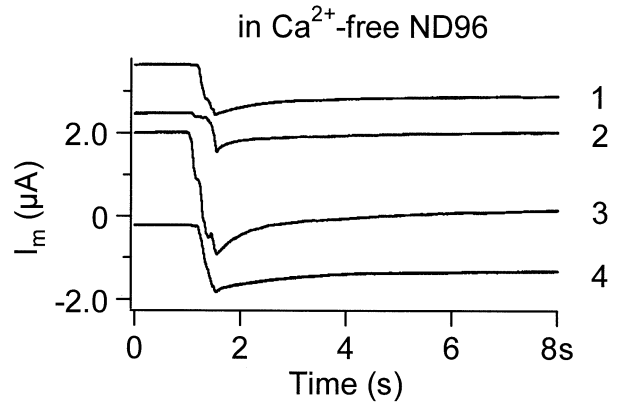
in Ca^{2+}-free ND96

Fig. 9. No resealing of the membrane in Ca^{2+}-free ND96. Consecutive current traces were recorded from the same oocyte under repeated tone-burst US irradiation of 0.29 MPa and 0.5-s duration. Numbers 1 to 4 indicate the sequence of recordings. Optison™ was introduced before each recording.

MHz in the presence of Optison™ from the recorded inward transmembrane current change. The current change during voltage clamp demonstrates an increase in cell membrane conductance, which indicates the increase of ion permeability across the cell membrane. The large current amplitude and the characteristic step-wise increase of current suggest that the ion permeability increase resulted from pore formation in the cell membrane (Hille 2001). These pores are not likely due to the increased opening of endogenous voltage or ligand-gated ion channels because, during US irradiation, the mem-

in ND96
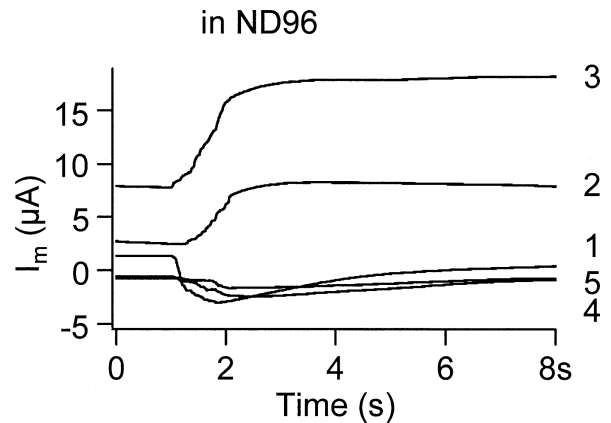
Fig. 10. Ca^{2+} entering the cell may be required for membrane resealing. The oocyte was bathed in ND96 and irradiated repeatedly with tone burst US of 0.29 MPa and 1-s duration. Membrane potential was clamped at either −50 or +50 mV. Numbers 1 to 5 indicate the sequence of recordings. The membrane potential at each recording was: 1 = −50 mV; 2 and 3 = consecutive recordings at +50 mV; 4 and 5 = consecutive recordings at −50 mV.

brane potential was clamped at a constant voltage and the solution bathing the oocyte contained no ligand known to activate endogenous ion channels. However, the size and shape of the pores are not known. In ion-selective ion channels, the pore size can be as small as $\sim$ 3 Å in diameter (Doyle et al. 1998; Zhou et al. 2001; Hille 2001). On the other hand, the step-wise increase of current could result from the formation of a single pore. Simply comparing the amplitude of the current step in our experiments ($\sim$ 0.1 μA, Fig. 7a) to the maximum current amplitude through a single K$^+$ channel ($\sim$ 100 pA) (Cui et al. 1997), and assuming that the current amplitude is only dependent on pore size, the US-induced pore can be as large as 0.1 μm. Such a rough estimation is based on a number of hypotheses. Nonetheless, it demonstrates the wide range that the US-induced pore size could be.

We observed that the inward transmembrane current increases after a delay of US activation and that the current reaches a maximum value at the end of US duration; the cell membrane subsequently recovers, indicated by the decay of the transmembrane current after US exposure. For US exposure with duration in the order of 1 s and pressure amplitude less than 1 MPa, the recovery time of sonoporation is on the order of 4 to 10 s. These values are comparable with the reported recovery rates for electroporation (Ryttsen et al. 2000; Barnett 1990). When the US pressure amplitude is high ($>$ 1 MPa), longer duration ($>$ 0.5 s) causes irreversible current increase, which indicates spontaneous cell death, confirmed by immediate microscopic examination.

Under our experimental conditions, we observed a distinct delay for the onset of transmembrane current increase after US activation in the presence of Optison™ (Fig. 4). In addition, the inward transmembrane current increases in a stepwise fashion during the US duration. The reported time for US destruction of Optison™ through fragmentation (Chomas et al. 2001; Dayton et al. 1999) or shell disruption/disintegration (Chomas et al. 2001; Dayton et al. 1999; Shi et al. 2000; Stride and Saffari 2003) ranges from a few μs to a few ms. The prolonged delay of sonoporation compared with the Optison™ destruction time indicates that the destruction of Optison™ does not immediately or directly cause sonoporation. It is unlikely that the delay and steps are caused by some intrinsic delayed response of the transmembrane current measurement to membrane status. This is clearly demonstrated by the absence of delayed response of transmembrane recovery at the end of the US exposure, indicating a spontaneous correspondence of the recorded transmembrane current to membrane status or pore formation.

Although we are planning to conduct further experimental studies to directly measure and monitor bubble activities during US exposure in the presence of Optison™ and other UCAs, we look for a possible explanation from the aspects of bubble dynamics and activities. As reported previously, fragmentation or destruction of Optison™ can generate secondary bubbles that can act as nuclei to induce subsequent bubble activities. The delay discussed above represents the time needed for sonoporation to occur induced by sufficient bubble activity that is generated after destruction of Optison™. Because during transient/inertial cavitation a bubble will grow to many times its equilibrium size and collapse rapidly within only a few cycles of US oscillation, transient/inertial cavitation unlikely originates directly from Optison™ destruction or immediately from the secondary bubble nuclei, based on our experimental observations. Therefore, possibly, these bubble nuclei may dissolve away into the solution due to dominating surface tension and gas diffusion. Some, however, may grow to larger sizes because of rectified diffusion (Crum 1984; Crum 1980; Church 1988) driven by a US field; or, the bubbles may coalesce with each other due to the secondary Bjerknes force (an attractive force between oscillating bubbles in a US field) (Crum 1975) to form larger bubbles. If they approach the resonant radius (Medwin 1977) corresponding to the frequency of the driving US field, these surviving or newly formed bubbles may collapse easily due to instability or inertia effect. Such bubble collapsing activity will then produce the next generation of multiple smaller bubbles, which may again grow or coalesce to form larger bubbles and initiate more bubble collapsing, possibly setting up cyclic bubble activities alternating between bubble growth and collapses (Neppiras 1980).

The characteristic stepwise fashion that the inward transmembrane current exhibited during US exposure was more clearly demonstrated in recordings using Ca^{2+}-free ND96 solution (Fig. 7a). The use of Ca^{2+}-free ND96 solution excluded currents flowing through endogenous Ca^{2+}-dependent Cl$^-$ channels that would have been activated by Ca^{2+} entering the cell during sonoporation (Miledi 1982; Barish 1983). During the step period, there were no sufficient bubble activities for sonoporation; therefore, the transmembrane current remained constant until the next synchronized bubble collapsed and induced additional membrane disruption, causing its further increase to a higher step level. Thus, the stepwise increases of the transmembrane current are an indication of sustained ongoing, yet cyclic, processes of bubble activities established during US irradiation. The steps are generally shorter at higher pressure levels (0.05 $\pm$ 0.25 s at 0.29 MPa, data not shown) and in less air-saturated (degassed for 30 min) solution, consistent with the trends observed for the delay.

We have observed that higher US pressures and/or longer durations (*e.g.,* 0.7 MPa for 0.5 s) in the presence of Optison™ caused large, irreversible increase in the transmembrane current, which appeared to correspond to spontaneous cell death observed in immediate post-US microscopic examinations. Reversible sonoporation occurred at low to moderate acoustic pressures (< 0.5 MPa), wherein pores formed during the US pulses and resealed after US exposure (0.01 to 1 s in our experiments) in ND96 solution (Figs. 8a and b) with a time course of 3 to 10 s, comparable with the recovery rates for electroporation (Ryttsen et al. 2000; Barnett 1990). However, the membrane did not show resealing after sonoporation in the Ca^{2+}-free ND96 solution (Fig. 9). The accumulated current increase shown at the beginning of each consecutive US exposure in Ca^{2+}-free ND96 (Fig. 9a) is in sharp contrast to the results in ND96 solution that all the current traces have similar starting levels (Fig. 8a). It was reported previously that, after application of laser-induced stress wave, the cell membrane increased permeability to calcein for a prolonged period of $\sim$ 80 s (Lee et al. 1996; Doukas and Flotte 1996) in a solution of Dulbecco phosphate-buffered saline (D-PBS) that did not contain Ca^{2+} (Lee et al. 1996). These results, of prolonged resealing process, are consistent with our observation that Ca^{2+} is essential for membrane resealing. Our additional experimental results (Fig. 10) further support the conclusion that Ca^{2+} must enter the cell for the membrane to reseal.

Under voltage clamp, the direction of current across the cell membrane, inward (negative in value) or outward (positive in value), depends on membrane potential set by the clamp, the equilibrium potentials of K^+ and Cl^- due to the opening of endogenous K^+ and Cl^- channels (Hille 2001) and nonspecific leaking currents. Electric currents across the membrane carried by K^+ and Cl^- change from outward to inward direction when membrane potential changes from above the equilibrium potential to below the equilibrium potential. The equilibrium potentials of K^+ and Cl^- in *Xenopus* oocytes range from -50 to -70 mV. Therefore, when the nonspecific leaking current is small (*e.g.,* before US irradiation), the membrane current usually flows outward and is of positive values when membrane potential is clamped at $\geq$ -50 mV (Figs. 9 and 10). US-induced pore formation increases nonspecific leaking currents, which have an equilibrium potential of $\sim$ 0 mV. Therefore, US irradiation induced an increase in inward current at membrane potential of -50 mV (Figs. 9 and 10) or outward current at membrane potential of $+50$ mV (Fig. 10).

Our preliminary study demonstrated that the novel application of electrophysiology methods, such as two-electrode voltage clamp techniques, allows us to study in real-time the cell response to US exposure. Monitoring and characterization of the dynamic cell sonoporation process provides important information with regard to the understanding of sonoporation mechanism. The parameters and observations can serve as necessary guidance for optimal design of US protocol for potential applications in drug and gene delivery.

Future studies are in planning to study sonoporation in mammalian cells. We will investigate the effects of US protocols such as pulse duration, duty cycle and pulse repetition frequency on sonoporation process and other cell effects. More direct measurement of cavitation and bubble dynamics will be employed to correlate such activities with the recordings in transmembrane current. More investigation is also planned to characterize the pore size in sonoporation and optimal conditions for drug/compound transport into the cell through the pores induced by sonoporation.

REFERENCES

Bao S, Thrall BD, Gies RA, Miller DL. In vivo transfection of melanoma cells by lithotripter shock waves. Cancer Res 1998;58:219–221.

Barish ME. A transient calcium-dependent chloride current in the immature Xenopus oocyte. J Physiol 1983;342:309–325.

Barnett A. The current-voltage relation of an aqueous pore in a lipid bilayer membrane. Biochim Biophys Acta 1990;1025:10–14.

Chomas JE, Dayton P, Allen J, Morgan K, Ferrara KW. Mechanisms of contrast agent destruction. IEEE Trans Ultrason Ferroelec Freq Control 2001;48:232–248.

Church CC. Prediction of rectified diffusion during nonlinear bubble pulsations at biomedical frequencies. J Acoust Soc Am 1988;83:2210–2217.

Crum LA. Bjerknes forces on bubbles in a stationary sound field. J Acoust Soc Am 1975;57:1363–1370.

Crum LA. Measurements of the growth of air bubbles by rectified diffusion. J Acoust Soc Am 1980;68:203–211.

Crum LA. Acoustic cavitation series: Part five, Rectified diffusion. Ultrasonics 1984;25:215–223.

Cui J, Cox DH, Aldrich RW. Intrinsic voltage dependence and Ca2+ regulation of mslo large conductance Ca-activated K+ channels. J Gen Physiol 1997;109:647–673.

Dayton PA, Morgan KE, Klibanov AL, Branderburger GH, Ferarra KW. Optical and acoustical observations of the effects of ultrasound on contrast agents. IEEE Trans UFFC 1999;46:220–232.

Doukas AG, Flotte TJ. Physical characteristics and biological effects of laser-induced stress waves. Ultrasound Med Biol 1996;22:151–164.

Doyle DA, Morais Cabral J, Pfuetzner RA, et al. The structure of the potassium channel: Molecular basis of K+ conduction and selectivity. Science 1998;280:69–77.

Feril LB Jr, Kondo T, Zhao QL, et al. Enhancement of ultrasound-induced apoptosis and cell lysis by echo contrast agents. Ultrasound Med Biol 2003;29:331–337.

Greenleaf WJ, Bolander ME, Sarkar G, Goldring MB, Greenleaf JF. Artificial cavitation nuclei significantly enhance acoustically induced cell transfection. Ultrasound Med Biol 1998;24:587–595.

Hille B. Ion channels of excitable membranes, 3rd ed. Sunderland, MA: Sinauer Associates, 2001.

Lee S, Anderson T, Zhang H, Flotte TJ, Doukas AG. Alteration of cell membrane by stress waves *in vitro*. Ultrasound Med Biol 1996;22:1285–1293.

Marmottant P, Hilgenfeldt S. Controlled vesicle deformation and lysis by single oscillating bubbles. Nature 2003;423:153–156.

Masu Y, Nakayama K, Tamaki H, et al. cDNA cloning of bovine substance-K receptor through oocyte expression system. Nature 1987;329:836–838.

Medwin H. Counting bubbles acoustically: A review. Ultrasonics 1977;15:7–13.

Miledi R. A calcium-dependent transient outward current in Xenopus laevis oocytes. Proc R Soc Lond B Biol Sci 1982;215:491–497.

Miller DL, Bao S, Gies RA, Thrall BD. Ultrasonic enhancement of gene transfection in murine melanoma tumors. Ultrasound Med Biol 1999;25:1425–1430.

Miller DL, Pislaru SV, Greenleaf JE. Sonoporation: mechanical DNA delivery by ultrasonic cavitation. Somat Cell Mol Genet 2002;27:115–134.

Neppiras EA. Acoustic cavitation thresholds and cyclic processes. Ultrasonics 1980;18:201–209.

Ryttsen F, Farre C, Brennan C, et al. Characterization of single-cell electroporation by using patch-clamp and fluorescence microscopy. Biophys J 2000;79:1993–2001.

Shi J, Krishnamoorthy G, Yang Y, et al. Mechanism of magnesium activation of calcium-activated potassium channels. Nature 2002;418:876–880.

Shi WT, Forsberg F, Tornes A, Ostensen J, Goldberg BB. Destruction of contrast microbubbles and the association with inertial cavitation. Ultrasound Med Biol 2000;26:1009–1019.

Stride E, Saffari N. On the destruction of microbubble ultrasound contrast agents. Ultrasound Med Biol 2003;29:563–573.

Stuhmer W. Electrophysiologic recordings from Xenopus oocytes. Methods Enzymol 1998;293:280–300.

Tachibana K, Uchida T, Ogawa K, Yamashita N, Tamura K. Induction of cell-membrane porosity by ultrasound. Lancet 1999;353:1409.

Ward M, Wu J, Chiu JF. Experimental study of the effects of Optison® concentration on sonoporation *in vitro*. Ultrasound Med Biol 2000;26:1169–1175.

Zhou Y, Morais-Cabral JH, Kaufman A, MacKinnon R. Chemistry of ion coordination and hydration revealed by a K+ channel-Fab complex at 2.0 A resolution. Nature 2001;414:43–48.